Giant electric-field-induced reversible and permanent magnetization reorientation on magnetoelectric Ni/(011) $[Pb(Mg_{1/3}Nb_{2/3})O_3]_{(1-x)}-[PbTiO_3]_x$ heterostructure

Tao Wu (吴涛),[1,a] Alexandre Bur,[1] Ping Zhao,[1] Kotekar P. Mohanchandra,[1] Kin Wong,[2] Kang L. Wang,[2] Christopher S. Lynch,[1] and Gregory P. Carman[1]
[1]*Department of Mechanical and Aerospace Engineering, University of California, Los Angeles, California 90095, USA*
[2]*Department of Electrical Engineering, University of California, Los Angeles, California 90095, USA*

(Received 15 October 2010; accepted 11 December 2010; published online 3 January 2011)

We report giant reversible and permanent magnetic anisotropy reorientation in a magnetoelectric polycrystalline Ni thin film and (011)-oriented $[Pb(Mg_{1/3}Nb_{2/3})O_3]_{(1-x)}-[PbTiO_3]_x$ heterostructure. The electric-field-induced magnetic anisotropy exhibits a 300 Oe anisotropy field and a 50% change in magnetic remanence. The important feature is that these changes in magnetization states are stable without the application of an electric field and can be reversibly switched by an electric field near a critical value ($\pm \boldsymbol{E}_{cr}$). This giant reversible and permanent magnetization change is due to remanent strain originating from a non-180° ferroelectric polarization reorientation when operating the ferroelectric substrate in a specific non-linear regime below the electric coercive field. © *2011 American Institute of Physics*. [doi:10.1063/1.3534788]

Multiferroic and magnetoelectric (ME) materials have attracted significant scientific interest due to the potential of electrically controlling magnetization properties.[1,2] Altering the magnetic states with an electric field has several important applications, such as spintronics[3,4] and magnetic random access memory (MRAM).[5,6] During the last decade, several studies have demonstrated electrically reversible magnetization change in magnetoelectric heterostructures.[7–12] These studies mainly use the linear ferroelectric response to induce temporary magnetization changes, i.e., the magnetization properties return to their initial states after the electric field is removed. Alternatively, mechanisms that produce a reversible and permanent magnetic anisotropy change (i.e., after releasing the electric field) are necessary for electrically writing nonvolatile bit information for MRAM applications. Therefore, a new approach is required to produce a permanent magnetic anisotropy change when the electric field is removed and reversible when the electric field is subsequently applied.

Chu *et al.*[13] demonstrated a permanent and reversible 90° magnetization rotation in ferromagnetic CoFe coupled with multiferroic $BiFeO_3$, relying on complex ferroelectric (FE), antiferromagnetic, and ferromagnetic interactions. Pertsev and Kohlstedt[14] and Hu *et al.*[15] proposed the concept of electric-field-induced 90° magnetization reorientation between two stable and orthogonal magnetic easy axes in a cubic magnetocrystalline structure. While promising, the experimental results have not yet been reported.

In this paper, we experimentally demonstrate a giant electric-field-induced reversible and permanent magnetization reorientation in a 35 nm polycrystalline Ni thin film using the nonlinear ferroelectric response of a (011) oriented single crystal $[Pb(Mg_{1/3}Nb_{2/3})O_3]_{(1-x)}-[PbTiO_3]_x$ (PMN-PT) ($x \approx 32\%$). Operating the PMN-PT in a specific nonlinear regime produces a large reversible remanent strain induced by non-180° polarization reorientation. This large remanent strain causes a permanent change in the magnetic anisotropy of the Ni thin film due to the magnetoelastic effect. This reversible and permanent magnetization change requires low operating electric fields (within ±0.2 MV/m), is highly repeatable, and is simple to implement.

Figure 1 illustrates the layered ME heterostructure and the rhombohedral crystal structure of (011) PMN-PT with eight possible ⟨111⟩ spontaneous polarization directions. 10 nm Ti and 50 nm Pt layers are deposited on both sides as electrodes. After poling the PMN-PT substrate, 5 nm Ti and 35 nm polycrystalline Ni films are deposited by e-beam evaporation. The magnetic properties of the Ni thin film are characterized using a longitudinal mode magnetooptical Kerr effect (MOKE) magnetometry.[15]

Figure 2(a) shows the electric displacement $\boldsymbol{D}$ as a function of the electric field $\boldsymbol{E}$ applied along the [011] direction for: (1) bipolar cycle within ±0.6 MV/m and (2) unipolar cycle from −0.14 to 0.6 MV/m. Figure 2(b) shows the cor-

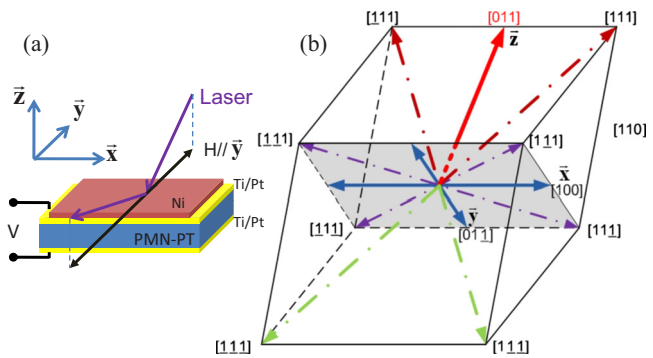

FIG. 1. (Color online) (a) Schematic of the heterostructure and the MOKE measurement; (b) Rhombohedral crystal structure of (011) PMN-PT structure with 8-possible ⟨111⟩ polarization directions. The dashed lines indicate the successive domain orientations during the polarization process: (1) stable $[\bar{1}11]/[111]$ or $[\bar{1}\bar{1}\bar{1}]/[1\bar{1}\bar{1}]$ states along poled $\vec{z}$ direction, (2) metastable $[\bar{1}\bar{1}\bar{1}]$, $[1\bar{1}\bar{1}]$, $[11\bar{1}]$, $[\bar{1}1\bar{1}]$ in-plane stables.

[a]Electronic mail: charlywu@ucla.edu.

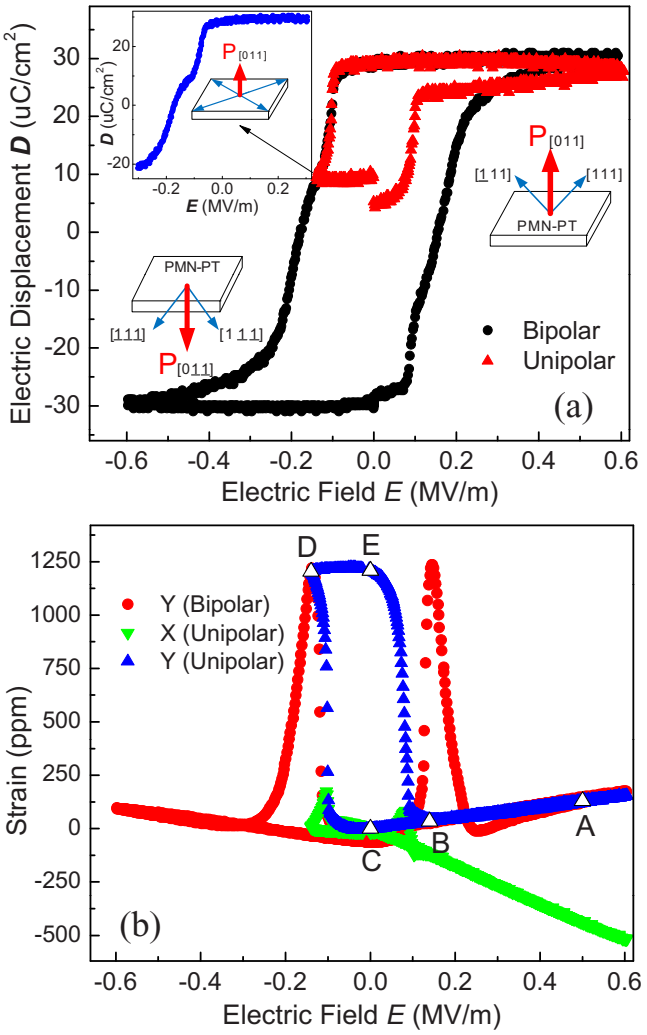

FIG. 2. (Color online) (a) Out-of-plane ($\bar{z}$ direction) electric displacement as a function of electric field. (b) In-plane piezoelectric strain value along the $\bar{\mathbf{x}}$ and $\bar{y}$ directions.

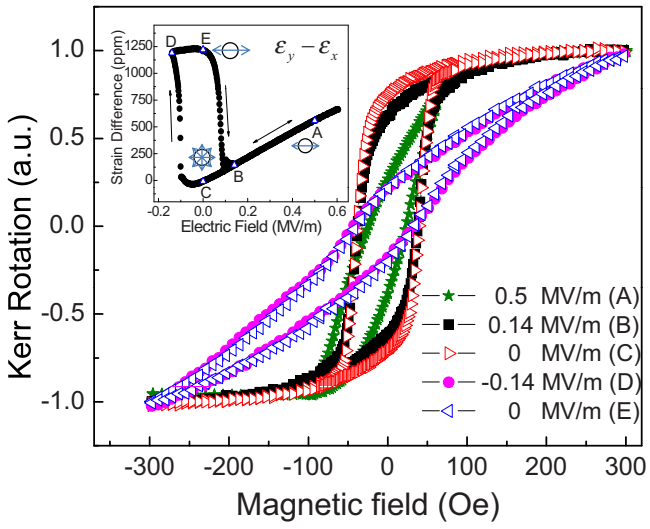

FIG. 3. (Color online) Normalized Kerr rotation hysteresis curves (***M-H***) along the $\bar{y}$ direction under different electric fields (letters are the representatives of the labeled strain states in the inset). The inset shows in-plane strain difference ($\varepsilon_y - \varepsilon_x$) as a function of electric field. The drawings indicate the magnetization state: (c) permanent easy plane, [(a) and (b)] temporary easy axis along $\bar{\mathbf{x}}$, and [(d) and (e)] permanent easy axis along $\bar{\mathbf{x}}$.

responding bipolar strain $\boldsymbol{\varepsilon}$ measured along $\bar{y}$ as well as unipolar strain curves measured along $\bar{x}$ and $\bar{y}$. The bipolar ***D-E*** curve in Fig. 2(a) shows a typical hysteresis curve with remanent polarization of 30 μC/cm^2 and coercive field $\boldsymbol{E}_c \approx 0.2$ MV/m. In contrast, the bipolar $\boldsymbol{\varepsilon}$-***E*** curve along $\bar{y}$ shown in Fig. 2(b) indicates a large nonlinear strain jump below the $\boldsymbol{E}_c$, which is attributed to non-180° FE polarization reorientation.[16–18] The material behavior is described with reference to Fig. 1(b). For specimens poled along the [011] $\bar{z}$ direction, there are roughly equal volume fractions of two crystal variants with polarizations aligned along the two [1̄11] and [111] variants. When a reversed electric field is applied ($-\boldsymbol{E}_c < \boldsymbol{E} < 0$ MV/m), the strain and electric displacement curves suggest that the polarizations first reorient by non-180° polarization reorientation to four possible in-plane ⟨111⟩ directions. This non-180° polarization reorientation produces a large jump in the strain along the $\bar{y}$ direction. With further increases in the reversed electric field ($\boldsymbol{E} < -\boldsymbol{E}_c$), the polarizations undergo another non-180° polarization reorientation to the two [1̄11] and [11̄1] variants. This two stage polarization reversal process is also consistent with the two-stage ***D-E*** curve as can be seen in the magnified image of the inset in Fig. 2(a). The inset shows the existence of a metastable state during the polarization reversal at a critical field $\boldsymbol{E}_{cr} \approx -0.14$ MV/m. By operating near the vicinity of the critical field $\boldsymbol{E}_{cr}$, it is possible to take advantage of the first non-180° polarization reorientation to produce two reversible and permanent remanent strain states having significantly different strain values.

Figure 2(b) shows the unipolar strain curves along $\bar{\mathbf{x}}$ and $\bar{y}$ for electric field cycled between −0.14 MV/m (i.e., near $\boldsymbol{E}_{cr}$) and 0.6 MV/m. Both $\bar{\mathbf{x}}$ and $\bar{y}$ curves consist of two distinct piezoelectric responses: a linear response (A-B-C) and a nonlinear hysteretic response (C-D-E-B-C). Operating in the linear region, the PMN-PT substrate exhibits highly anisotropic response. The nonlinear hysteretic region exhibits two stable states with a large strain difference along $\bar{y}$. When a negative electric field is applied from 0 to $\boldsymbol{E}_{cr}$ (point C to point D), the strain response basically follows the bipolar strain curve with a large nonlinear strain jump at point D. This corresponds to the first non-180° polarization reorientation. As can be seen in the figure, removing the electric field at $\boldsymbol{E}_{cr}$ provides a stable large remanent strain of +1220 ppm along $\bar{y}$ (point E), while a small remanent strain of −18 ppm present along $\bar{\mathbf{x}}$. When a positive electric field is applied from 0 to +0.14 MV/m (point E to point B), the piezoelectric strain response jumps back to the original linear path (A-B-C), due to non-180° polarization reorientation. Here, when the electric field is removed, the remanent strain vanishes, thus the first non-180° polarization reorientation has been used to produce two reversible and permanent remanent strain states having significantly different strain values at E = 0 MV/m. The process described above can also be observed in the unipolar ***D-E*** curve provided in Fig. 2(a). The small gap shown in Fig. 2(a) at zero electric field is attributed to charging from the series capacitor in the Sawyer–Tower circuitry. It is important to note that the strain hysteresis loop (C-D-E-B-C) Fig. 2(b) is highly repeatable and stable without reductions in remanent strains at zero electric field.

Figure 3 shows the normalized Kerr hysteresis curves (***M-H***) of the Ni thin film on the PMN-PT substrate mea-

sured along $\bar{y}$ for different constant electric fields. Since the magnetic anisotropy of Ni thin film coupled with a FE substrate is dominated by the relative in-plane strain difference,[12] the inset of Fig. 3 plots the relative strain difference $(\varepsilon_y - \varepsilon_x)$ as a function of electric field measured from the unipolar $\boldsymbol{\varepsilon_x}$-$\boldsymbol{E}$ and $\boldsymbol{\varepsilon_y}$-$\boldsymbol{E}$ curves presented in Fig. 2(b). The applied electric fields in Fig. 3 are representative of the labeled strain states in the inset, i.e., (A) +0.5, (B) +0.14, (C) 0, (D) −0.14, and (E) 0 MV/m. For as-deposited Ni thin film, i.e., with 0 MV/m at point C, the magnetization of the film is predominantly in-plane, without a preferred axis of magnetization (isotropic easy-plane) as illustrated in the pictorial insert of Fig. 3 inset at point C. The $\boldsymbol{M}$-$\boldsymbol{H}$ hysteresis curve for point C shows a large remanent magnetization $(\boldsymbol{M}_r/\boldsymbol{M}_s > 90\%)$. If an electric field is applied in the linear ferroelectric regime (A-B-C), the $\boldsymbol{M}$-$\boldsymbol{H}$ curves shift from an initial high $\boldsymbol{M}_r/\boldsymbol{M}_s$ hysteretic curve to a low $\boldsymbol{M}_r/\boldsymbol{M}_s$ hysteretic curve, similar to previous published studies.[10,12] However, this magnetic anisotropy change for either point A or point B is temporary and the magnetization properties return to the initial isotropic easy plane after the electric field is released (i.e., returns to point C). A distinctly different result is observed when operating in the nonlinear regime (C-D-E-B-C).

As the electric field is decreased from 0 MV/m to $\boldsymbol{E}_{cr}$ at point D, the PMN-PT undergoes the first non-180° polarization reorientation, inducing a large strain at $\boldsymbol{E}_{cr}$. The large strain at point D produces a magnetic anisotropy in the Ni film with an easy axis along $\bar{\mathbf{x}}$ and a hard axis along $\bar{y}$ (see pictorial insert of Fig. 3 inset). At the electric field $\boldsymbol{E}_{cr}$ (point D), the Ni layer has a low remanence $(\boldsymbol{M}_r/\boldsymbol{M}_s < 25\%)$ and a large anisotropy field $\boldsymbol{H}_a = 300$ Oe along $\bar{y}$. More importantly, when the electric field is removed (point E), the strain remains and the magnetic anisotropy is permanently retained. This permanent change can be observed from the overlapped $\boldsymbol{M}$-$\boldsymbol{H}$ curves in Fig. 3 for points D and E. Therefore, a permanent magnetization reorientation has been achieved. To demonstrate reversibility, the electric field is now increased from 0 to +0.14 MV/m (point B), another non-180° polarization reorientation occurs back to the original poling directions, removing the remanent strain. When the electric field is removed, the strain value returns to point C and the Ni magnetization state returns to the original isotropic magnetization state. By cycling through this strain hysteresis loop (C-D-E-B-C), the magnetization state of Ni thin film can be positioned at two stable states (i.e., points E and C at Fig. 3) after applying and releasing two opposite electric fields $(\pm\boldsymbol{E}_{cr})$.

In conclusion we have demonstrated reversible and permanent change in the magnetic anisotropy in ME heterostructures. Operating the ferroelectric (011) PMN-PT in the nonlinear regime generates a reversible remanent strain in the ferroelectric layer, creating a reversible and permanent magnetic anisotropy in the Ni film. This approach provides an additional degree of freedom in the design of spintronics and MRAM devices.

The first two authors contributed equally. The authors appreciate Mr. Joshua L. Hockel, Michael C. Emmons, Chin-Jui Hsu, Hyungsuk K. D. Kim, and Scott Keller for their valuable discussion. This work was supported by the Air Force Office of Scientific Research (AFOSR) under Grant No. FA9550-09-1-0677, managed by Byung-Lip (Les) Lee, and the Swiss National Science Foundation (SNF) under Grant No. PBNEP2-124323.

[1] W. Eerenstein, N. D. Mathur, and J. F. Scott, Nature (London) **442**, 759 (2006).
[2] R. Ramesh and N. A. Spaldin, Nature Mater. **6**, 21 (2007).
[3] C. Binek, A. Hochstrat, X. Chen, P. Borisov, W. Kleemann, and B. Doudin, J. Appl. Phys. **97**, 10C514 (2005).
[4] A. Khitun, M. Bao, and K. Wang, IEEE Trans. Magn. **44**, 2141 (2008).
[5] M. Bibes and A. Barthelemy, Nature Mater. **7**, 425 (2008).
[6] Z. Li, J. Wang, Y. Lin, and C. W. Nan, Appl. Phys. Lett. **96**, 162505 (2010).
[7] M. Liu, O. Obi, J. Lou, Y. Chen, Z. Cai, S. Stoute, M. Espanol, M. Lew, X. Situ, K. S. Ziemer, V. G. Harris, and N. X. Sun, Adv. Funct. Mater. **19**, 1826 (2009).
[8] J. J. Yang, Y. G. Zhao, H. F. Tian, L. B. Luo, H. Y. Zhang, Y. J. He, and H. S. Luo, Appl. Phys. Lett. **94**, 212504 (2009).
[9] T.-K. Chung, S. Keller, and G. P. Carman, Appl. Phys. Lett. **94**, 132501 (2009).
[10] M. Liu, O. Obi, Z. Cai, J. Lou, G. Yang, K. S. Ziemer, and N. X. Sun, J. Appl. Phys. **107**, 073916 (2010).
[11] J. Das, M. Li, S. S. Kalarickal, S. Altmannshofer, K. S. Buchanan, J. F. Li, and D. Viehland, Appl. Phys. Lett. **96**, 222508 (2010).
[12] T. Wu, A. Bur, J. L. Hockel, K. Wong, T.-K. Chung, and G. P. Carman, "Electrical and Mechanical Manipulation of Ferromagnetic Properties in Polycrystalline Nickel Thin Film," IEEE Magn. Lett. (submitted).
[13] Y.-H. Chu, L. W. Martin, M. B. Holcomb, M. Gajek, S.-J. Han, Q. He, N. Balke, C.-H. Yang, D. Lee, W. Hu, Q. Zhan, P.-L. Yang, A. Fraile-Rodriguez, A. Scholl, S. X. Wang, and R. Ramesh, Nature Mater. **7**, 478 (2008).
[14] N. A. Pertsev and H. Kohlstedt, Appl. Phys. Lett. **95**, 163503 (2009).
[15] J.-M. Hu, Z. Li, J. Wang, and C. W. Nan, J. Appl. Phys. **107**, 093912 (2010).
[16] H. Fu and R. Cohen, Nature (London) **403**, 281 (2000).
[17] G. Yiping, H. Luo, H. Tianhou, X. Haiqing, and Y. Zhiwen, Jpn. J. Appl. Phys., Part 1 **41**, 1451 (2002).
[18] T. Liu and C. S. Lynch, Acta Mater. **51**, 407 (2003).